Theor Chem Acc (2016) 135:256
DOI 10.1007/s00214-016-2007-5

REGULAR ARTICLE

Smooth models for the Coulomb potential

Cristina E. González-Espinoza[1] · **Paul W. Ayers**[1] · **Jacek Karwowski**[2] · **Andreas Savin**[3]

Received: 22 June 2016 / Accepted: 30 September 2016 / Published online: 31 October 2016

Abstract Smooth model potentials with parameters selected to reproduce the spectrum of one-electron atoms are used to approximate the singular Coulomb potential. Even when the potentials do not mimic the Coulomb singularity, much of the spectrum is reproduced within the chemical accuracy. For the hydrogen atom, the smooth approximations to the Coulomb potential are more accurate for higher angular momentum states. The transferability of the model potentials from an attractive interaction (hydrogen atom) to a repulsive one (Harmonium and the uniform electron gas) is discussed.

Keywords Model potentials · Hydrogen spectra · Harmonium

1 Philosophy

How feasible is it to find a model for the Coulomb interaction that is easier to evaluate but still reproduces key properties of the physical interaction? A logical starting point is a system with *no interaction*, as in Kohn–Sham density functional theory (DFT) [1]. The Kohn–Sham (KS) approximation starts from a non-interacting system, described as the sum of the individual electrons' contributions to the energy:

$$\hat{H}_s = \sum_i^N \left(-\frac{1}{2}\nabla_i^2 + v_s(r_i) \right). \tag{1}$$

In order to ameliorate the effect of omitting the Coulomb repulsion between the electrons, an extra term, the exchange-correlation functional $E_{xc}[\rho]$, is introduced into the energy expression. For a given external potential $v(r)$

$$E_v[\rho] = T_s[\rho] + J[\rho] + E_{xc}[\rho] + \int v(r)\rho(r)\mathrm{d}r, \tag{2}$$

where $T_s[\rho]$ is the kinetic energy functional of the non-interacting system, $J[\rho]$ is the classical repulsion and $E_{xc}[\rho]$ is the exchange-correlation functional, which must be approximated [2]. The Euler–Lagrange equation associated with the stationary condition of $E_v[\rho]$ can be transformed into a self-consistent set of equations:

$$\begin{aligned} &\left(-\frac{1}{2}\nabla^2 + v(r) + \int \frac{\rho(r')}{|r-r'|}\mathrm{d}r' + v_{xc}(r) - \epsilon_j \right)\phi_j(r) = 0 \\ &\rho(r) = \sum_{j=1}^N \left|\phi_j(r)\right|^2 \\ &v_{xc}(r) = \frac{\delta E_{xc}[\rho(r)]}{\delta\rho(r)}. \end{aligned} \tag{3}$$

Published as part of the special collection of articles "Festschrift in honour of A. Vela".

✉ Paul W. Ayers
ayers@mcmaster.ca

Cristina E. González-Espinoza
gonzalce@mcmaster.ca

Jacek Karwowski
jka@fizyka.umk.pl

Andreas Savin
andreas.savin@lct.jussieu.fr

[1] McMaster University, 1280 Main Street West, Hamilton, ON L8S4L8, Canada

[2] Institute of Physics, Nicolaus Copernicus University, 87-100 Toruń, Poland

[3] Laboratoire de Chimie Théorique, UMR7616, CNRS and UPMC, Sorbonne Universités, F-75252 Paris, France

In principle, the KS solutions are exact when E_{xc} is exact, and the KS orbitals yield the exact density of the system with N electrons in the external potential $v(r)$. The accuracy of KS density functional approximations (DFA) depends on the approximation one uses for E_{xc}. The simplest approximation is the local density approximation (LDA) [3–5]. In LDA, it is assumed that the exchange-correlation functional is local,

$$E_{xc}[\rho(r)] = \int \epsilon_{xc}(\rho(r))\mathrm{d}r, \tag{4}$$

where the exchange-correlation energy density $\epsilon_{xc}(\rho(r))$ at r is taken from the uniform electron gas with density $\rho(r)$.

To accurately recover the effect of omitting the interaction between the electrons, one constructs an adiabatic connection that links the KS *non-interacting* system with the physical *interacting* system. Traditionally, this adiabatic connection is written as a function of the strength of the interaction, using a simple multiplicative factor λ [6–9]:

$$\hat{H}_\lambda = \sum_{i=0}^{N} -\frac{\nabla_i^2}{2} + v_\lambda(r_i) + \frac{1}{2}\sum_{j\neq i}\frac{\lambda}{r_{ij}}. \tag{5}$$

Computational studies of the adiabatic connection have been performed for few-electron atomic systems and provide significant insight into the structure of the exact exchange-correlation density functional [10–16]. An alternative to the traditional adiabatic connection is to write the Coulomb interaction as the sum of a short-range piece and a long-range piece. The long-range piece of the potential is usually chosen to be smooth (or at least non-singular), so that it is relatively easy to approximate solutions to the Schrödinger equations when only the long-range piece is included.

So far we have reviewed traditional strategies that add density functional corrections to an "easy" system to approximate the real system. Can we use the real system to construct the model? For example, is it possible to select an interaction potential, different from the Coulomb one, that nonetheless reproduces a certain target property of the system? For example, one might wish to select an interaction potential that preserves the energy spectrum of an atom. This strategy is not new. Valance and Bergeron [17] show how to construct analytically solvable pseudopotentials and model potentials, in the framework of supersymmetric quantum mechanics, that reproduce experimental spectra. Starting from a one-electron one-dimensional Hamiltonian H_1 associated with the potential V_1, they found a supersymmetric partner H_2, characterized by a second potential V_2, with almost the same spectrum as H_1. H_2 is missing the ground state of H_1. A similar approach has been used by Lepage [18] in the field of elementary particle physics, where the Hamiltonian is constructed to reproduce low-energy features of a particular physical system.

In the next section, we define an expression for the model potential. We then explain two different model potentials that accurately reproduce the lowest energy eigenvalues of the hydrogen atom. In Sect. 4, we use the same models for the Coulomb potential to replace the Coulomb repulsion between the electrons in two-electron Harmonium. Finally, the exchange energy of the uniform electron gas that results from one of the models is compared to the standard approximation.

2 Ansatz

Analogous to the inverse problem of finding the Kohn–Sham potential from a given density, where oscillatory potentials and/or shifted potentials can reproduce the exact density numerically [19], finding the potential given the spectrum is not trivial because the solution is not unique. Therefore, we restrict the analytical form of the potential by imposing some constraints. We would like to eliminate the singularity of the Coulomb potential because solving the Schrödinger equation for a singular operator is computationally demanding. We also wish to preserve the long-range asymptotic form of the potential, so that the long-range electrostatics is correct. An interaction potential that satisfies these constraints is:

$$\frac{1}{r} \rightarrow V_\mu(r) = c\,\exp\left(-\alpha^2 r^2\right) + \frac{\mathrm{erf}(\mu r)}{r}. \tag{6}$$

We prove in this article that despite the simplicity of this *erfgau* [20] type of potential, it is flexible enough for our purposes.

3 H atom

3.1 Construction of $V_\mu(r)$

To determine the parameters in the model potential, we consider what happens when we replace the Coulomb interaction between the nucleus and the electron in the hydrogen atom by the model potential $V_\mu(r)$ (6). Thus, we replace the Hamiltonian of the hydrogen atom

$$\hat{H}_0(\mathbf{r}) = -\frac{1}{2}\nabla^2 - \frac{1}{r} \tag{7}$$

by a modified Hamiltonian

$$\hat{H}_\mu(\mathbf{r}) = -\frac{1}{2}\nabla^2 - V_\mu(r) \tag{8}$$

with $V_\mu(r)$ defined in such a way that

$$\lim_{\mu\to\infty} \hat{H}_\mu = \hat{H}_0, \quad \text{i.e.} \quad \lim_{\mu\to\infty} V_\mu = \frac{1}{r}. \tag{9}$$

As we know, in the case of the long-range term

$$\frac{\operatorname{erf}(\mu\, r)}{r} \underset{\mu\to\infty}{\sim} \frac{1}{r}.$$

Thus, condition (9) is fulfilled if $[c\,\exp(-\alpha^2 r^2)] \to 0$ when $\mu \to \infty$. Besides, we would like the spectrum of $\hat{H}_\mu$ to be as close as possible to the spectrum of $\hat{H}_0$. This can be achieved by properly choosing $c = c(\mu)$ and $\alpha = \alpha(\mu)$.

Consider $\hat{H}_0$ as the unperturbed operator, and

$$w_\mu = \hat{H}_\mu - \hat{H}_0 \tag{10}$$

as a perturbation. First, we notice that for the bound states of the hydrogen atom

$$\langle \psi_i | \operatorname{erfc}(\mu\, r)/r | \psi_i \rangle \underset{\mu\to\infty}{\sim} \mu^{-(2l+2)}, \tag{11}$$

and

$$\left\langle \psi_i | c\, \exp\left(-\alpha^2 r^2\right) | \psi_i \right\rangle \underset{\alpha\to\infty}{\sim} c\, \alpha^{-(2l+3)}, \tag{12}$$

where l is the angular momentum quantum number, a necessary condition for the spectra of $\hat{H}_\mu$ and $\hat{H}_0$ to coincide is that these two expectation values have the same asymptotic form. (See "Appendix 1" for more details about the μ-dependence of the wavefunction.) The simplest choice, adopted in this paper, is to take α as a linear function of μ. This implies that c also has to be linear in μ. Thus, we can set

$$c = \gamma\, \mu, \qquad \alpha = \kappa\, \mu, \tag{13}$$

where γ and κ are μ-independent parameters.

According to Eqs. (11), (12) and (13), the asymptotic expansion of the expectation value of w_μ may be written as

$$\langle \psi_i | w_\mu | \psi_i \rangle = \sum_{j=2l+2} d_j(\gamma, \kappa)\, \mu^{-j}, \quad \mu >> 1. \tag{14}$$

We select γ and κ so that the two leading terms in expansion (14) vanish. The lowest order terms ($j = 2$ and $j = 3$) correspond to $l = 0$ states. For angular momenta $l > 0$ the leading terms in Eq. (14) are $O(\mu^{-4})$ or smaller. Then, the choice of $c(\mu)$ and $\alpha(\mu)$ is dictated by the requirement that the eigenvalues of the S states are as correct as possible for $\mu \to \infty$. The explicit form of expansion (14) for $l = 0$ states reads (see "Appendix 2")

$$\left\langle \psi_i | w_\mu | \psi_i \right\rangle = \left(1 - \frac{\sqrt{\pi}\gamma}{\kappa^3}\right)\mu^{-2} + \left(-\frac{8}{3\sqrt{\pi}} + \frac{4\gamma}{\kappa^4}\right) \times \mu^{-3} + O\left(\mu^{-4}\right). \tag{15}$$

Solving equations $d_2 = d_3 = 0$ for γ and κ, we obtain:

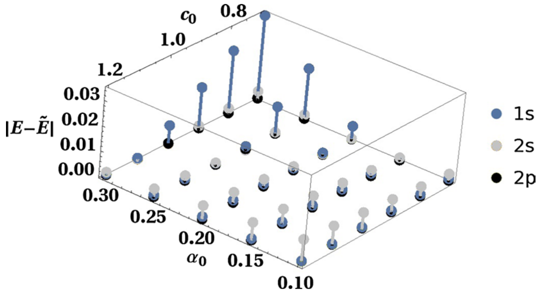

Fig. 1 Accuracy of the model potential spectrum with respect to the parameters c_0 and α_0. Energy errors (in %), for $\mu = 1$

$$c = \frac{27}{8\sqrt{\pi}}\,\mu\ = 1.904\,\mu, \qquad \alpha = \frac{3}{2}\,\mu\ = 1.500\,\mu. \tag{16}$$

In addition to the asymptotic behavior, for practical calculations we need the optimal parameters c and α at finite values of μ. Taking the linear forms

$$c = \gamma\,\mu + c_0, \qquad \alpha = \kappa\,\mu + \alpha_0 \tag{17}$$

with the parameter γ and κ from the previous step we can use c_0 and α_0 to further optimize the spectrum. The condition for the elimination of μ^{-2} term remains the same as before. The equations $d_3 = 0$ and $d_4 = 0$ are given in "Appendix 2." The behavior of the spectrum of the model potential versus c_0 and α_0 is shown in Fig. 1, where for fixed $\mu = 1.0$ energies of $1s$, $2s$ and $2p$ states are displayed. As one can see, there is a range for which pairs of (c_0, α_0) give reasonably small errors of the energy values. The dependence of the relative error on n and l is discussed in Sect. 3.2.2.

To select the best linear forms of c and α we constructed a grid on the intervals $c = [-0.5, 0.0]$ and $\alpha = [1.0, 3.0]$, and then, we computed the error in the eigenvalues of the $1s$, $2s$, $2p$, $3s$, $3p$ and $3d$ states for $\mu = [0.5, 2.0]$. We defined the best choice for the parameters as the minimax choice: the c, α that minimized the maximum absolute deviation between the eigenvalues with the model potential and the exact result from the Coulomb interaction,

$$\delta = \min_{c(\mu),\alpha(\mu)} \left\{ \max_{n,l} |E_{\text{Coulomb}} - E_{\text{model}}| \right\}. \tag{18}$$

As seen in Fig. 2, the best values of (c, α) can be modeled by a linear function,

$$\begin{aligned} c &= 0.923 + 1.568\,\mu \\ \alpha &= 0.241 + 1.405\,\mu. \end{aligned} \tag{19}$$

Note that the resulting fit is very similar to one the linear forms obtained from perturbation theory $\{c_0 = 0.943, \gamma = 1.904\,\mu\}$ and $\{\alpha_0 = 0.247, \kappa = 1.5\,\mu\}$ [see Eq. (52) of "Appendix 2"]. With this fitted form, the interaction does not vanish when $\mu = 0$; therefore, the spectrum cannot be

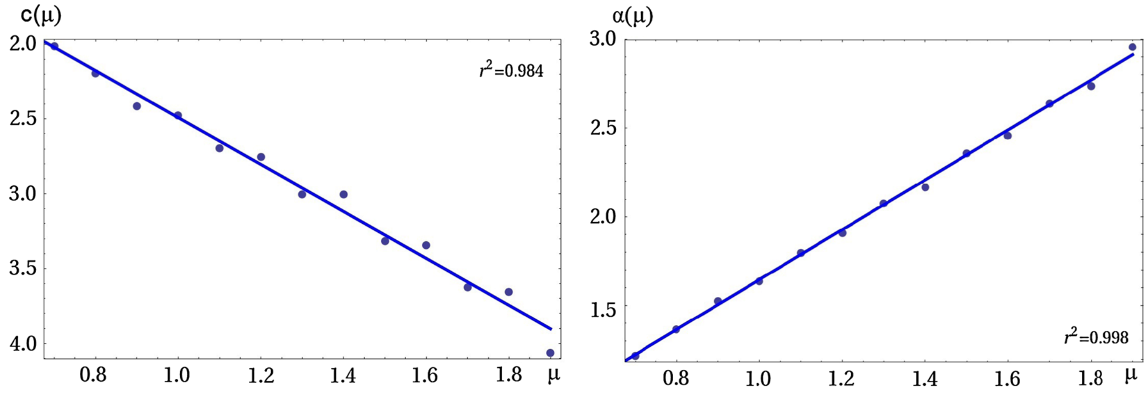

Fig. 2 Linear regressions for the two parameters $c(\mu)$ and $\alpha(\mu)$ of the simple fit in Eq. (19). Here, the *dots* are the optimal values of the parameters according to Eq. (18), the *lines* are the least squares linear regressions, and r^2 are their corresponding coefficients of determination

exact for small values of μ, in contrast to the asymptotic form (16), in which both c and α are proportional to μ.

The optimum parameters for a hydrogen-like atom with the nuclear charge Z may be obtained from the ones determined for the case of $Z = 1$ by a simple scaling procedure. Equation (6) becomes

$$\frac{Z}{r} \to V_\mu^Z(r) = Z\left[c_Z \exp\left(-\alpha_Z^2 r^2\right) + \frac{\operatorname{erf}(\mu_Z r)}{r}\right] \tag{20}$$

and

$$\hat{H}_\mu^Z(\boldsymbol{r}) = -\frac{1}{2}\nabla^2 - V_\mu^Z(r) = Z^2\,\hat{H}_\mu(\boldsymbol{\rho}), \tag{21}$$

where $\boldsymbol{\rho} = Z\,\boldsymbol{r}$ and

$$c_Z = Z\,c, \quad \alpha_Z = Z\,\alpha, \quad \mu_Z = Z\,\mu. \tag{22}$$

3.2 Results

3.2.1 Potentials

The model potentials we consider in this paper [$\operatorname{erf}(\mu r)/r$, asymptotic Eq. (16), and fitted Eq. (19)] corresponding to $\mu = 1$ are compared with the Coulomb potential and with a modified long-range potential, $\operatorname{erf}(3r)/r$, in Fig. 3. One might suspect that adding an optimized Gaussian term to $\operatorname{erf}(\mu r)/r$ would give a potential that mimics the effect of increasing μ in the long-range term. This is not the case for the potentials we consider in this paper. At first glance, the potential $\operatorname{erf}(3r)/r$ (dashed line) seems similar to the asymptotic and to the fitted potentials. But the $\operatorname{erf}(3r)/r$ potential is *always* weaker than the Coulomb potential, while the latter potentials, though in some intervals of r are also weaker, in other intervals are stronger than the Coulomb potential. This may explain why the asymptotic and fitted potentials reproduce the spectrum much better than the modified long-range potential: The effects of too strong and too weak regions of the model potentials cancel each other, leaving the eigenvalues relatively unchanged.

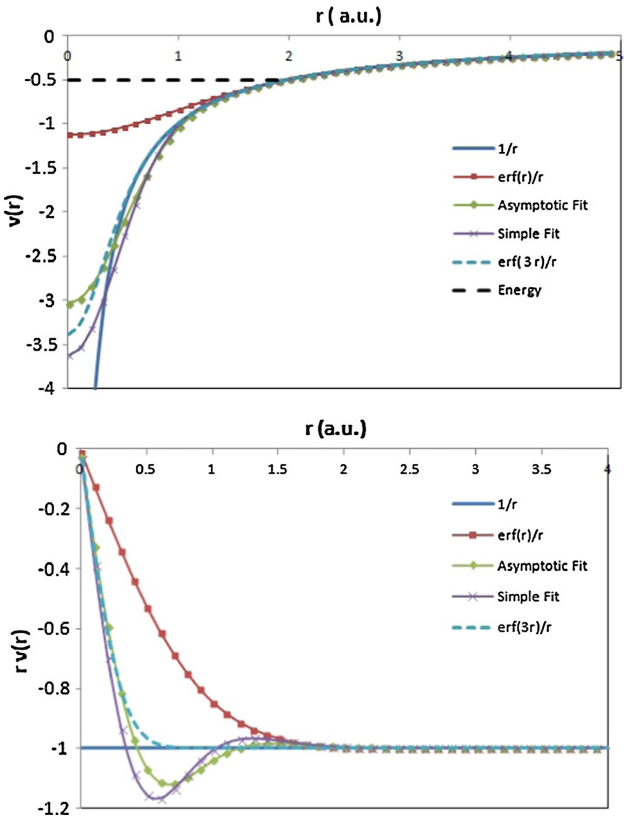

Fig. 3 Comparison between the Coulomb potential (*solid line*) and the model potentials: long-range (*squares*), asymptotic (*diamonds*), fitted (*stars*) and modified long-range potential (*dashed line*)

3.2.2 Eigenvalues

The percentage errors in the eigenvalues of hydrogen with long-range, asymptotic and fitted potentials are presented

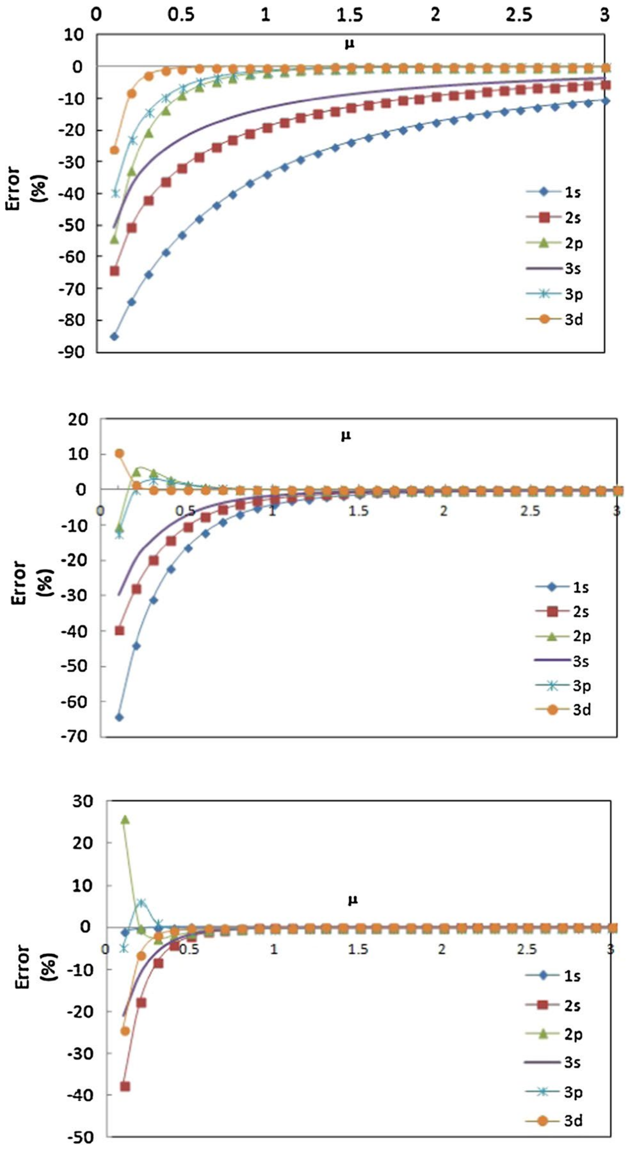

Fig. 4 Percentage errors in the eigenvalues of hydrogen. From *top* to *bottom*: **a** long-range $\operatorname{erf}(\mu r)/r$, **b** asymptotic [Eq. (16)], and **c** fitted [Eq. (19)] potentials

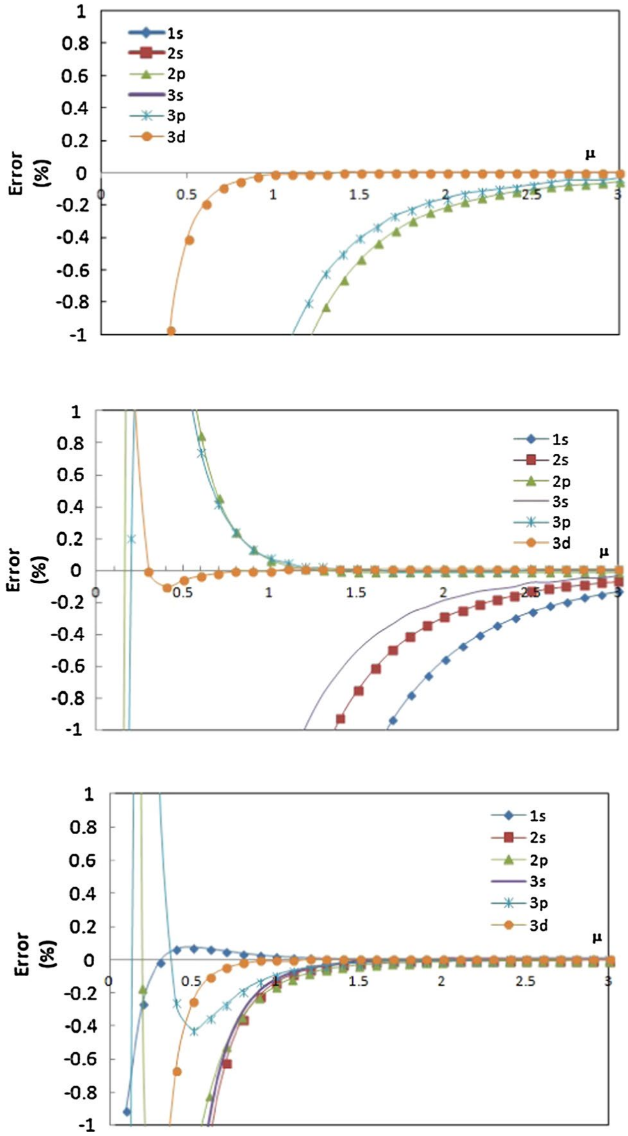

Fig. 5 Close-up of the percentage error of the eigenvalues of hydrogen. As in Fig. 4, the *curves* are, from *top* to *bottom*: **a** long-range $\operatorname{erf}(\mu r)/r$, **b** asymptotic [Eq. (16)], and **c** fitted [Eq. (19)] potentials

in Fig. 4. As the quantum number increases, the amplitude of the eigenfunctions near the nucleus decreases, the long-range part of the potential dominates and the eigenvalues approach the exact ones. A clear improvement is found in the asymptotic and fitted potentials compared with the traditional long-range potential. As expected, the fitted potential produced the smallest errors. However, for $\mu > 1.5$, the difference between the asymptotic and the fitted models is rather small; see Fig. 5.

The advantage of adding a Gaussian term is clear when we compare against a modified long-range potential, such as $\operatorname{erf}(3\mu r)/r$, Fig. 6. The Gaussian term lets us "get away with" a much smaller value of μ and seems to work better for s-type orbitals than the erf-based potential.

As expected from the asymptotic analysis, better results are obtained for higher angular momentum because the centrifugal barrier, $l(l+1)/2r^2$, pushes the electron away from the nucleus, into a region where the difference between the model potential and the Coulomb potential is negligible (see Figs. 7, 8). On the other hand, when μ is close to zero, the eigenvalues from the model potential are very poor, because the short-range Gaussian term cannot bind an electron when the angular momentum is too high. When we look at the wavefuntion, for example, the $1s$ and

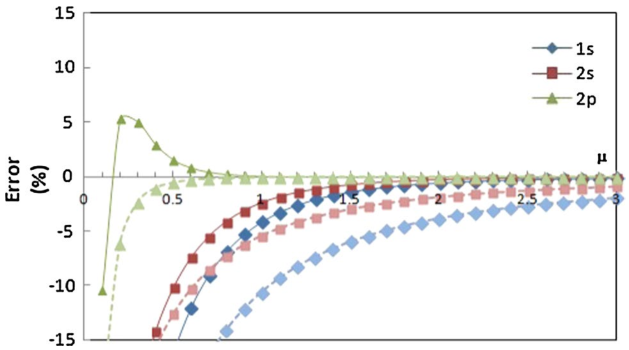

Fig. 6 Comparison of the percent error in the first three eigenvalues of the hydrogen atom between the asymptotic potential, (*thick lines*) and erf$(3\,\mu)/r$ (*dashed lines*)

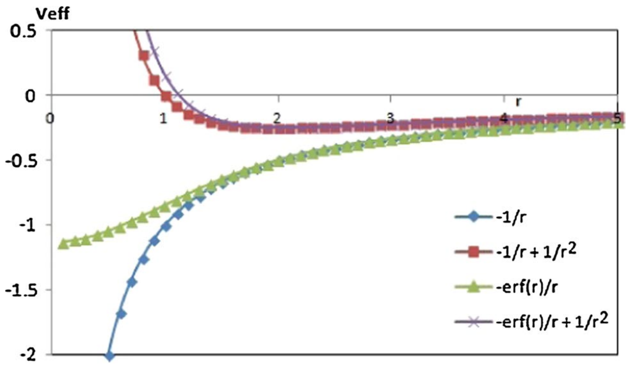

Fig. 7 Comparison between the radial potentials $-1/r$ and $-\mathrm{erf}(r)/r$ in the hydrogen atom, when $l = 0$ (*diamonds* and *squares*, respectively) and $l = 1$ (*triangles* and *stars*)

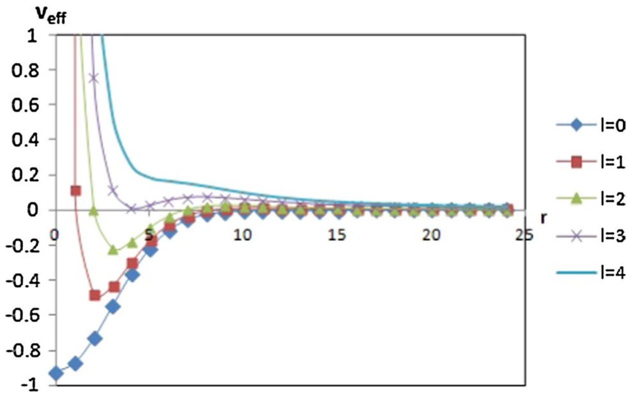

Fig. 8 Effect of the centrifugal term on the radial potential in the $\mu \to 0$ limit for the fitted erfgau interaction [Eq. (19)]

2*s* orbitals (Fig. 9), we see that even though the eigenvalues are very similar, the eigenfunctions can be quite different.

How important is this difference? Is the perturbation still small if spectrum is nearly reproduced? Moreover, can we use the same approach for other types of interactions, e.g., a repulsive potential? There are several ways to assess the transferability of our model potentials. Below we use the same replacement for the electron–electron repulsion in two model systems, Harmonium and the uniform electron gas.

4 Harmonium

To explore whether the model potentials can be used to describe repulsive interactions, we consider a system of two interacting electrons confined in a harmonic oscillator potential, called Harmonium [21, 22]. The Hamiltonian of Harmonium is:

$$\hat{H}^{\mathrm{h}}(\mathbf{r}_1, \mathbf{r}_2) = -\frac{1}{2}\nabla_1^2 + \frac{\omega^2\, r_1^2}{2} - \frac{1}{2}\nabla_2^2 + \frac{\omega^2\, r_2^2}{2} + \frac{1}{|\mathbf{r}_1 - \mathbf{r}_2|}, \tag{23}$$

where the superscript h stands for *harmonium*. This Hamiltonian is separable if one rewrites it in terms of the center of mass and the relative coordinates

$$\mathbf{R} = \frac{1}{2}(\mathbf{r}_1 + \mathbf{r}_2), \quad \mathbf{r} = \mathbf{r}_1 - \mathbf{r}_2. \tag{24}$$

In the new coordinates

$$\hat{H}^{\mathrm{h}}(\mathbf{r}_1, \mathbf{r}_2) = \hat{H}^{\mathrm{h}}_{\mathbf{r}}(\mathbf{r}) + \hat{H}^{\mathrm{h}}_{\mathbf{R}}(\mathbf{R}), \tag{25}$$

where

$$\hat{H}^{\mathrm{h}}_{\mathbf{r}}(\mathbf{r}) = -\nabla_{\mathbf{r}}^2 + \frac{\omega^2\, r^2}{4} + \frac{1}{r}, \tag{26}$$

$$\hat{H}^{\mathrm{h}}_{\mathbf{R}}(\mathbf{R}) = -\frac{1}{4}\nabla_{\mathbf{R}}^2 + \omega^2\, R^2 \tag{27}$$

and the Schrödinger equation separates into two equations:

$$\hat{H}^{\mathrm{h}}_{\mathbf{r}}(\mathbf{r})\, \Phi_{\mathrm{nlm}}(\mathbf{r}) = \epsilon_{nl}\, \Phi_{\mathrm{nlm}}(\mathbf{r}) \tag{28}$$

and

$$\hat{H}^{\mathrm{h}}_{\mathbf{R}}(\mathbf{R})\, \xi_{\nu\lambda\mu}(\mathbf{R}) = \eta_{\nu\lambda}\, \xi_{\nu\lambda\mu}(\mathbf{R}), \tag{29}$$

where n, l, m and ν, λ, μ are quantum numbers, and the total energy is equal to $E_{\nu\lambda;nl} = \eta_{\nu\lambda} + \epsilon_{nl}$.

In the case of Harmonium, we can use the same approximation for the Coulomb potential as we did for the hydrogen atom, but now, instead of the *attractive* Coulomb interaction we have the *repulsive* one. Thus, the modified Hamiltonian for the relative motion of two electrons reads

$$\hat{H}^{\mathrm{h}}_{\mathbf{r};\mu}(\mathbf{r}) = -\nabla_{\mathbf{r}}^2 + \frac{\omega^2\, r^2}{4} + V_\mu(r). \tag{30}$$

Due to the spherical symmetry, it is convenient to express the solutions of Eqs. (28) and (29) in spherical coordinates. In particular, if we set

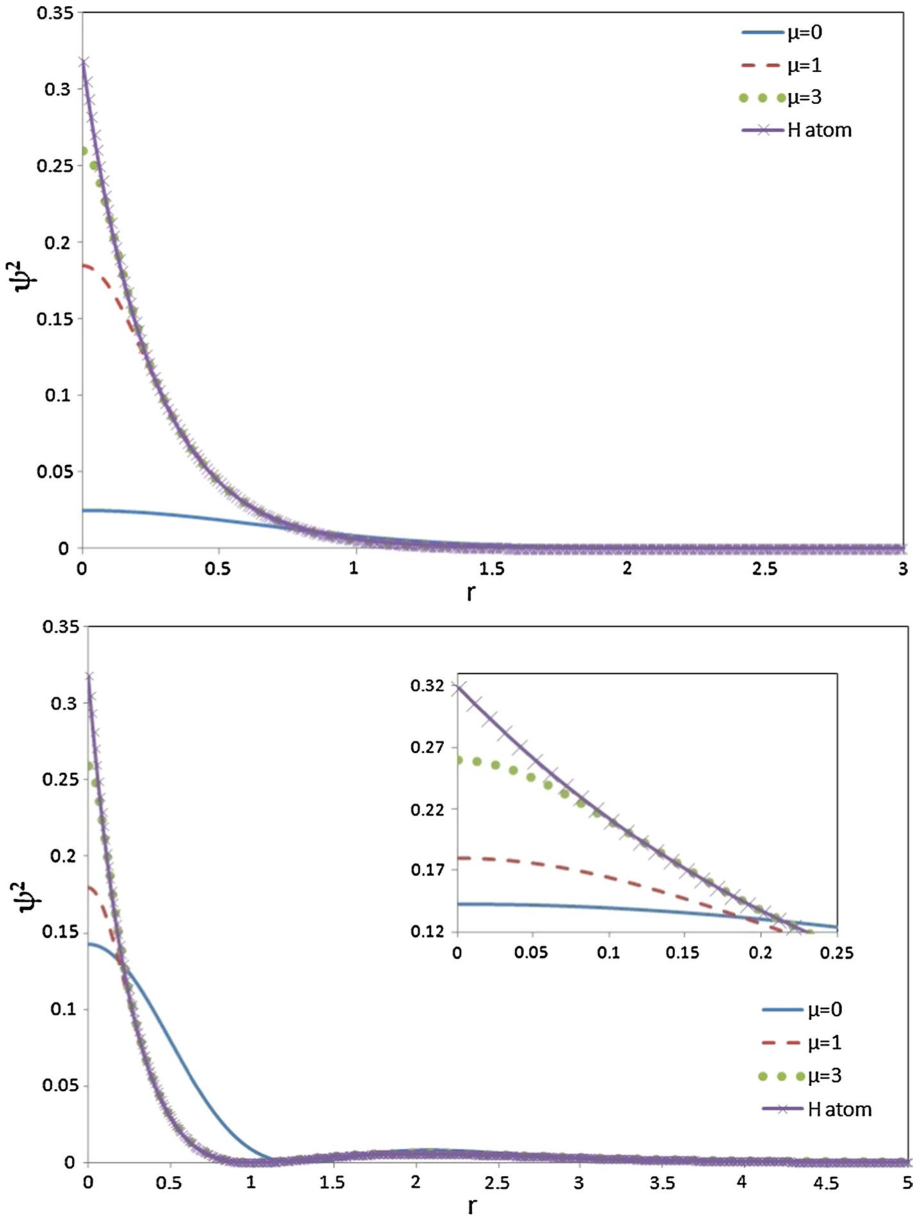

Fig. 9 Orbital densities $|\psi_{1s}(r)|^2$ (*top*) and $|\psi_{2s}(r)|^2$ (*bottom*) derived from the model Hamiltonian of hydrogen, Eq. (8) with $c = 0.923 + 1.568\,\mu$, $\alpha = 0.241 + 1.405\,\mu$, using different values of μ

$$\Phi_{\mathrm{nlm}}(\mathbf{r}) = \frac{1}{r}\,\phi_{nl}(r)\,Y_{lm}(\hat{r}), \tag{31}$$

where $Y_{lm}(\hat{r})$ are spherical harmonics, then in the case of Eq. (28) with the modified Hamiltonian (30) we have

$$\left[-\frac{\mathrm{d}^2}{\mathrm{d}r^2} + \frac{l(l+1)}{r^2} + \frac{\omega^2\,r^2}{4} + V_\mu(r)\right]\phi_{nl}(r) = \epsilon_{nl}\,\phi_{nl}(r). \tag{32}$$

4.1 How Harmonium is computed

In order to assess the model potentials for Harmonium, we solved Eq. (32) numerically. To this end, we discretized this equation on a grid of N equidistant points for $r \in [0, a]$ with the boundary conditions $\phi_{nl}(0) = \phi_{nl}(a) = 0$ and the approximation

$$\frac{d^2}{dr^2}\,\phi_{nl}(r) \approx \frac{1}{h^2}[\phi_{nl}(r-h) - 2\phi_{nl}(r) + \phi_{nl}(r+h)],$$

where $h = a/N$. The discretized equation may be written as

$$\sum_{j=0}^{N}\left(A_{ij} - \epsilon_{nl}\,\delta_{ij}\right)\phi_{nl}(r_j) = 0,$$

where $r_j = j\,h$, $j = 0, 1, \ldots, N$ and

$$A_{ij} = \left(\frac{2}{h^2} + \frac{l(l+1)}{r_j^2} + \frac{\omega^2\,r_j^2}{4} + V_\mu(r_j)\right)\delta_{ij} - \frac{\delta_{i,j+1} + \delta_{i,j-1}}{h^2}$$

It has been solved using standard LAPACK subroutines. In the calculations, we set $N = 10{,}000$ and $a = 10/\omega$. In order to discard errors due to the numerical procedure, we computed and compared the eigenvalues of two states for which we know the analytic solution:

$$\begin{aligned} &\phi_1 \sim r^{l+1}(1 + \omega r)\mathrm{e}^{-\omega r^2/4}, \quad \omega = \frac{1}{2(l+1)}, \\ &\quad E_1 = \omega\left(l + \frac{5}{2}\right) \end{aligned} \tag{33}$$

and

$$\begin{aligned} &\phi_2 \sim r^{l+1}\left[1 + \frac{r(1+\omega r)}{2(l+1)}\right]\mathrm{e}^{-\omega r^2/4}, \quad \omega = \frac{1}{2(4l+5)}, \\ &\quad E_2 = \omega\left(l + \frac{7}{2}\right). \end{aligned} \tag{34}$$

For $l = 0$, the percentage errors in the eigenvalues obtained with the numerical integration are $5.76 \times 10^{-6}\%$ and $6.52 \times 10^{-6}\%$, respectively.

4.2 Results

In Fig. 10, the eigenvalues of Harmonium with $n = 1$ and $l = 0$ are shown for the long-range, asymptotic and fitted potentials. Similar to the hydrogen atom, a deterioration at small μ is observed, but now the asymptotic potential is slightly better than the fit to the hydrogenic spectrum, and both are much better than the uncorrected $\mathrm{erf}(\mu r)/r$ potential. As the harmonic confinement weakens ($\omega \to 0$), the average distance between electrons increases, and the models become more accurate because of their correct 1 / r asymptotics. For strongly confined electrons ($\omega >> 1$), however, the Gaussian correction factors that were adapted to the hydrogenic spectrum do not seem appropriate for modeling the short-range 1 / r interaction. In Table 1, we collected the smallest value of μ such that the error is always <1%, for the different values of ω. It is clear that as the range of the average distance between the electrons decreases ($\omega \to \infty$), we also need to scale the range separation parameter ($\mu \to 0$).

In order to investigate the interplay between the strength of confinement and the parameters of the model potential, let us scale the variable in Eq. (28) with Hamiltonian (30) to reduce the confinement parameter to $\omega = 1$. After the substitution $\rho = \sqrt{\omega}\, r$. We get

$$\begin{aligned} &\left[-\nabla_\rho^2 + \frac{\rho^2}{4} + \frac{1}{\sqrt{\omega}}\left(\frac{\mathrm{erf}(\tilde{\mu}\rho)}{\rho} + \tilde{c}\,\mathrm{e}^{-\tilde{\alpha}^2\rho^2}\right)\right] \\ &\quad \phi_{nl}(\rho) = \tilde{\epsilon}_{nl}\phi_{nl}(\rho), \end{aligned} \tag{35}$$

where

$$\tilde{c} = c/\sqrt{\omega}, \quad \tilde{\alpha} = \alpha/\sqrt{\omega}, \quad \tilde{\mu} = \mu/\sqrt{\omega}, \quad \tilde{\epsilon}_{nl} = \epsilon_{nl}/\omega. \tag{36}$$

Thus, to compensate for changing ω we have to properly scale parameters and multiply the potential by $\sqrt{\omega}$. In Fig. 11, we can see that by appropriately scaling the parameters of the model potential we get, for all values of ω, exactly the same energies.

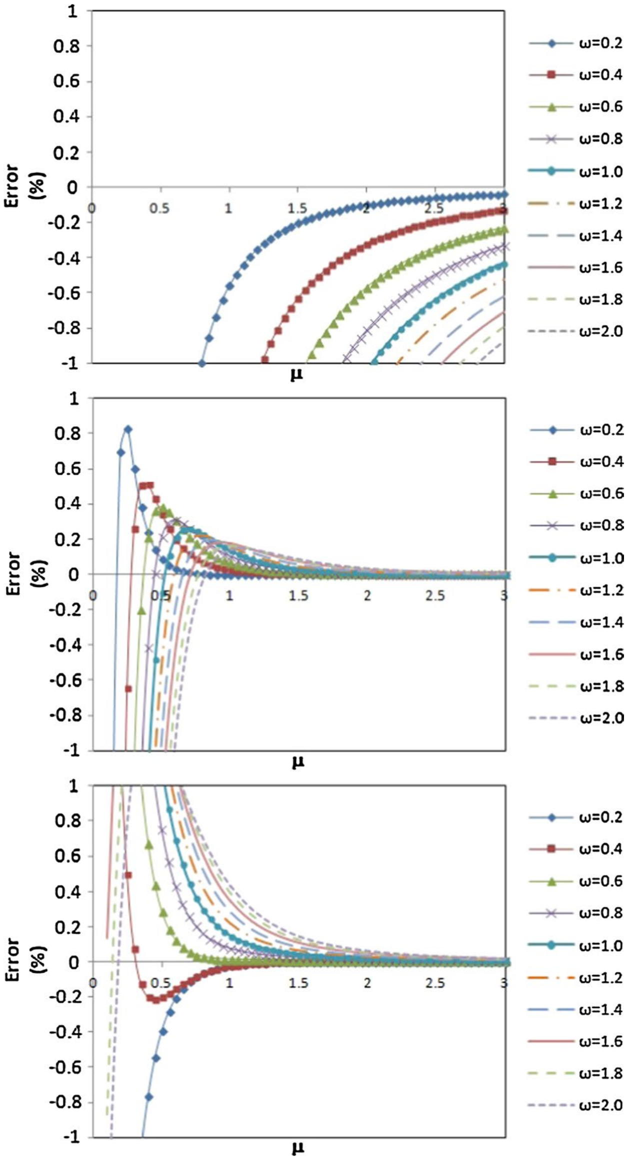

Fig. 10 Errors (in %) of the Harmonium eigenvalues as function of μ, for different ω. From *top* to *bottom*: **a** long-range $\mathrm{erf}(\mu r)/r$, **b** asymptotic (Eq. 16), and **c** fitted (Eq. 19) potentials

To show that the same method can be used for excited states, we computed the excitation energy from the ground state to the first excited $l = 0$ state, using the long-range, $\mathrm{erf}(3\mu r)/r$, asymptotic and fitted potentials (see Fig. 12). There is some cancelation of errors (i.e., the energy spacing is better than the absolute energy), but the results are still

Table 1 Smallest value of the range parameter μ needed to obtain a percentage error <1% with the model potentials for Harmonium, for a given value of ω

ω	0.2	0.4	0.6	0.8	1.0	1.2	1.4	1.6	1.8	2.0
Asymptotic	0.2	0.25	0.35	0.4	0.45	0.5	0.5	0.55	0.6	0.6
Fitted	0.4	0.25	0.4	0.5	0.55	0.6	0.65	0.65	0.65	0.65

poor for small values of μ, confirming that the parameters in the model potential should be ω-dependent. We should note, however, that the erfgau potential with fixed parameters is still much better than the raw $\mathrm{erf}(\mu r)/r$ potential.

5 Uniform electron gas

We now examine the effect of using a modified potential on the energy of the uniform electron gas. Consider the Hartree–Fock energy of the N-particle spin-unpolarized uniform electron gas confined in the volume Ω with density $\rho = N/\Omega$, in the limit where N and Ω go to infinity at constant ρ. The one-electron reduced density matrix has the well-known form [23]

$$\gamma(\mathbf{r}, \mathbf{r}') = 3\rho \frac{\sin(x) - x\cos(x)}{x^3}, \quad \text{with } x = k_F |\mathbf{r} - \mathbf{r}'|, \tag{37}$$

which is not affected when we replace the Coulomb interaction, both attractive and repulsive, with the modified interaction (Eq. 6), because it depends only on the Fermi wave number $k_F = (3\pi^2\rho)^{1/3}$. Furthermore, the compensation of the electrostatic terms is maintained (*i.e.*, the electrostatic contribution sums up to zero, just as in the standard case). However, the exchange energy is modified to

$$E_x = -\frac{1}{2} \int \int \mathrm{d}\mathbf{r}\, \mathrm{d}\mathbf{r}'\, \gamma\left(\mathbf{r}, \mathbf{r}'\right)^2 V_\mu\left(\left|\mathbf{r} - \mathbf{r}'\right|\right). \tag{38}$$

Using $\int \rho\, d\mathbf{r} = N$ and transforming the variables of integration, one obtains

$$E_x = -\frac{6}{\pi^2} N \int_0^\infty x^2 \left(\frac{\sin(x) - x\cos(x)}{x^3}\right)^2 V_\mu\left(\frac{x}{k_F}\right) \mathrm{d}x. \tag{39}$$

Replacing V_μ with the erfgau form of interest to us, Eq. (6), we can then separate the integral into two terms, the Gaussian function term and the error function term

$$\begin{aligned} &\int_0^\infty x^2 \left(\frac{\sin(x) - x\cos(x)}{x^3}\right)^2 V_\mu\left(\frac{x}{k_F}\right) \mathrm{d}x \\ &\quad = \int_0^\infty x^2 \left(\frac{\sin(x) - x\cos(x)}{x^3}\right)^2 c\, e^{-\alpha^2\left(\frac{x}{k_F}\right)^2} \mathrm{d}x \\ &\qquad + \int_0^\infty x^2 \left(\frac{\sin(x) - x\cos(x)}{x^3}\right)^2 \frac{\mathrm{erf}\left(\mu \frac{x}{k_F}\right)}{\frac{x}{k_F}} \mathrm{d}x. \end{aligned} \tag{40}$$

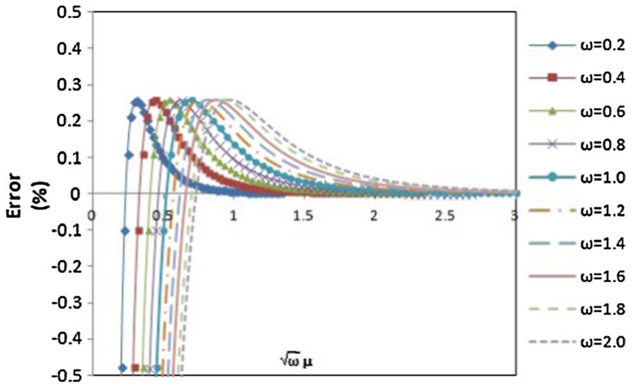

Fig. 11 Errors (in %) of the Harmonium eigenvalues as function of $\sqrt{\omega}\mu$, for different ω using the scaled asymptotic [Eq. (16)] potential

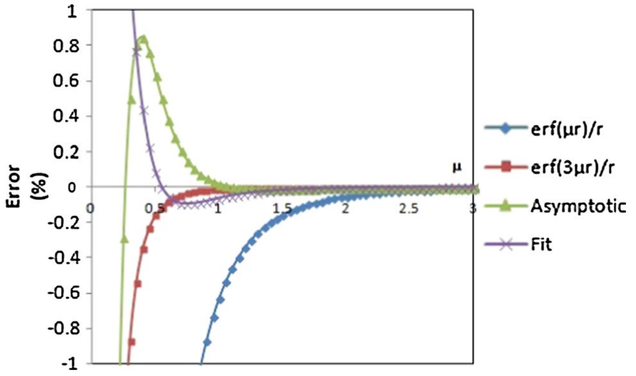

Fig. 12 Errors (in %) of the excitation energy to the first excited $l = 0$ state of Harmonium, as function of μ, for $\omega = 1$. Long-range $\mathrm{erf}(\mu r)/r$ (*diamonds*), $\mathrm{erf}(3\mu r)/r$ (*squares*), asymptotic [Eq. (16)] (*triangles*) and fitted [Eq. (19)] (*stars*) potentials

Both integrals can be easily evaluated using standard tools for numerical computations such as Mathematica [24].

In Fig. 13, we show the exchange energy per particle $\epsilon_x = E_x/N$, as function of μ and the density parameter $r_s = (3/4\pi\,\rho)^3$, using the asymptotic potential (Eq. 16). We observe that the model works well for large $\mu\, r_s$, but it does not seem possible to correct the interaction at short range. Here, it is important to notice the similarity with Harmonium. As ω controls the distance between the electrons, r_s describes the electron density distribution. A small value of ω translates to short interparticle distances, making the gas "denser," and as consequence, difficult to describe with the

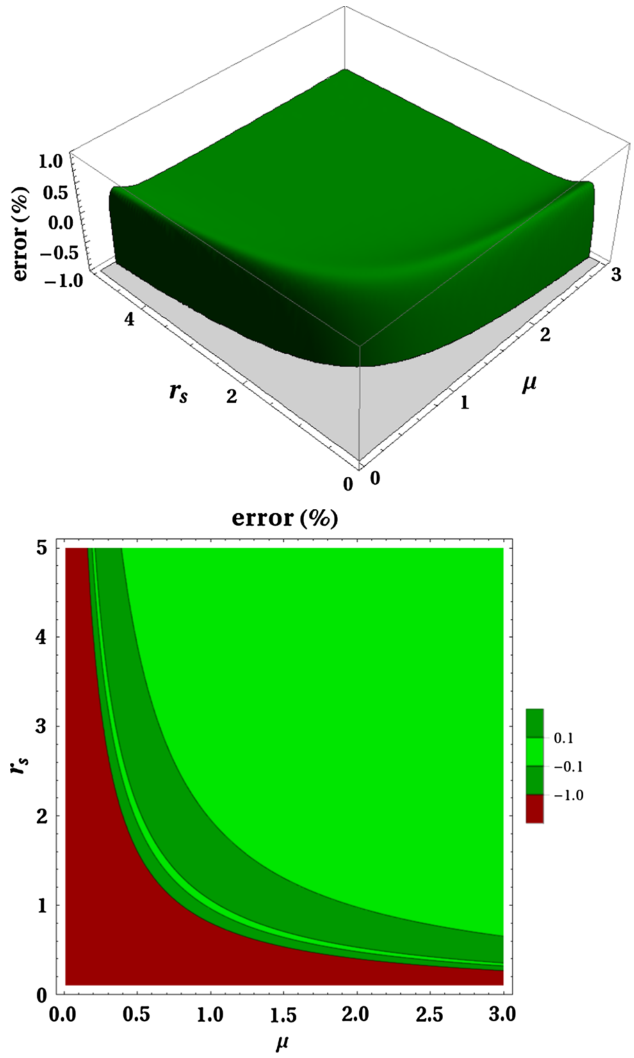

Fig. 13 Error (in %) in $\epsilon_x(r_s, \mu)$, for the uniform electron gas using the model asymptotic potential (Eq. 16)

smooth potentials. This indicates that the optimal value of μ, just as in Harmonium, depends on the range of the interaction, r_s, so μ should be system-dependent.

6 Summary

Is it possible to replace the Coulomb potential with another potential that is computationally more convenient and, if so, how should the approximate potential be constructed? In this work, we examine whether adding a Gaussian function improves the performance of the traditional $\mathrm{erf}(\mu r)/r$ potential used in range-separated DFT. As the measure of the correctness of the model potential, we have chosen the difference between the spectra of the hydrogen atom calculated using the Coulomb potential and the modified one. It appears that for a reasonable range of parameters defining the new potential not only can the spectrum of the hydrogen atom be accurately reproduced, but using the same potential to replace the *repulsive* Coulomb potential in the Harmonium atom gives a significant improvement over the uncorrected $\mathrm{erf}(\mu r)/r$ potential.

The remaining question is whether one could somehow correct the residual error in the new potential. One way to do this would be to, as in range-separated DFT, use a correction functional for the neglected short-range contributions to the exchange-correlation energy. However, this biases one's treatment toward the ground-state energy and electron density: A different (and certainly much harder to construct) functional would be needed to correct other properties (e.g., excited-state properties) of the system. There is another way, however: The results of a few calculations at sufficiently large values of μ can be extrapolated to the physical $\mu \to \infty$ limit. This approach is applicable to any property, not just those that are readily accessible from KS DFT. Furthermore, replacing the electron–electron repulsion potential with a smooth function has major computational advantages, as it allows one to use smaller basis sets, with fewer polarization functions.

There are also cases where it may be favorable to replace the Coulombic electron–nucleus interaction with a model potential like those considered in this paper. For example, these smoothed Coulomb potentials could be used, instead of pseudopotentials, for diffusion quantum Monte Carlo and plane-wave DFT calculations. In those cases, the procedure would be the same: The system would be solved for several choices of the smoothed electron–nucleus interaction, and the results then extrapolated to the physical $\mu \to \infty$ limit.

Acknowledgements CEGE acknowledges CONACyT and the Secretariat of Innovation, Science and Technology of the State of Morelos for the scholarship for graduate studies, and MITACS for funding her visit to the Laboratoire de Chimie Théorique, where this work was initiated. PWA acknowledges support from NSERC and Compute Canada. This paper is dedicated to Alberto Vela, on the occasion of his sixtieth birthday. Alberto likes to improve results through understanding, rather than haphazardly. We find this trait admirable and worthy of imitation, and hope that through this paper we provide a better understanding of how to model electron interactions.

Appendix 1: Hydrogenic atoms: μ dependence and integrals' scaling.

The leading term in the hydrogenic radial function is

$$R_{nl}(r)^2 \sim Z^3 (Zr)^{2l} \mathrm{e}^{-2Zr/n}, \tag{41}$$

therefore

$$R_{nl}(r)^2 r^2 \mathrm{d}r \sim \rho^{2l+2} \mathrm{e}^{-2\rho/n} \mathrm{d}\rho \tag{42}$$

where $\rho = Zr$. Now, let

$$I(\mu) = \int_0^\infty f(\mu r) R_{nl}(r)^2 r^2 \mathrm{d}r \tag{43}$$

then

$$\begin{aligned} I(\mu) &\sim \int_0^\infty f\left(\frac{\mu\rho}{Z}\right)\rho^{2l+2}\mathrm{e}^{-2\rho/n}\mathrm{d}\rho \\ &= \left(\frac{Z}{\mu}\right)^{2l+3}\int_0^\infty f(x)x^{2l+2}\mathrm{e}^{-2Zx/\mu n}\mathrm{d}x \\ &= \left(\frac{Z}{\mu}\right)^{2l+3}\sum_{i=0}^\infty a_i\left(\frac{Z}{\mu}\right)^i, \end{aligned} \tag{44}$$

where $x = \mu\rho/Z$ and

$$a_i = \frac{(-1)^i}{i!}\left(\frac{2}{n}\right)^i \int_0^\infty f(x)x^{2l+i+2}\mathrm{d}x. \tag{45}$$

For $f(\mu r/Z) = \mathrm{erf}(\mu r)/Zr$, $f(x) = (\mu/Z)\mathrm{erf}(x)/x$ and the power of the asymptotic term is $(2l+2)$.

Appendix 2: Model Hamiltonian from first-order perturbation theory

We define the model Hamiltonian as

$$\hat{H}_\mu = -\frac{1}{2}\nabla^2 - \left[c\ \exp\left(-\alpha^2 r^2\right) + \frac{\mathrm{erf}(\mu\, r)}{r}\right], \tag{46}$$

where the parameters c and α should be chosen so that the eigenvalues of this operator are as close as possible to the ones of the physical operator,

$$\hat{H}_0 = -\frac{1}{2}\nabla^2 - \frac{1}{r}. \tag{47}$$

The difference between the two operators

$$w_\mu = \hat{H}_\mu - \hat{H}_0 = \frac{\mathrm{erfc}(\mu\, r)}{r} - c\exp\left(-\alpha^2 r^2\right) \tag{48}$$

is treated as a perturbation. We want the perturbation to vanish as $\mu \to \infty$. Moreover, we would like to keep a single parameter, μ, and make c and α functions of μ. As we mentioned in Sect. 3.1, one way to produce $\langle\psi_i|w_\mu|\psi_i\rangle = 0$ is to choose α increasing with μ. When we expand the expectation value of w_μ for large values of α and μ we obtain, for $l = 0$ states, the integrals of the hydrogenic functions $\psi_{n0} = \{4e^{-r},\ (2-r)e^{-r/2},\ \frac{4}{729}(27-18r+2r^2)e^{-r/3}\}$ are

$$\left\langle\psi_{n0}|w_\mu|\psi_{n0}\right\rangle = n^{-3}[A(\alpha,c) + B(\mu)] + O\left(\mu^{-5}\right), \tag{49}$$

where

$$A(\alpha,c) = -\frac{c\sqrt{\pi}}{\alpha^3} + \frac{4c}{\alpha^4}$$

comes from $\langle\psi_{n0}|c\ \exp(-\alpha^2 r^2)|\psi_{n0}\rangle$ and

$$B(\mu) = \frac{1}{\mu^2} - \frac{8}{3\sqrt{\pi}\mu^3} + \frac{3}{2\mu^4},$$

from $\langle\psi_{n0}|\mathrm{erfc}(\mu r)/r|\psi_{n0}\rangle$. Note that we used arbitrary multiplicative factors (4, 1 and $\frac{4}{729}$ respectively) to simplify the expressions. We can use this trick because we want to equate all expressions to 0.

In order to eliminate terms of order μ^{-2}, we set $\sqrt{\pi}\, c\,\alpha^{-3} = \mu^{-2}$. This means that $c = \gamma\,\mu$, $\alpha = \kappa\,\mu$ and $\gamma = \kappa^3/\sqrt{\pi}$. Substituting these values into the expansion (49) corresponding to $n = 1$, we see that the coefficient of μ^{-3} vanishes if $\gamma = (2\,\kappa^4)/(3\sqrt{\pi})$. From the last two equations, we get

$$\gamma = \frac{27}{8\sqrt{\pi}}, \quad \kappa = \frac{3}{2}$$

for which the energy of the S states is correct up to μ^{-4}. To eliminate the error for μ^{-4}, we would need to consider corrections from second-order perturbation theory. For $l = 1$, the expansion of the expectation value of w_μ starts with terms proportional to μ^{-4} and, in general, for an arbitrary l, the leading term of the expansion is proportional to $\mu^{-(2l+2)}$.

Now, let us consider the expansion of the expectation values of w_μ for the linear forms $\alpha = \kappa\mu + \alpha_0$ and $c = \gamma\mu + c_0$ with the parameter γ and κ from the previous step. The condition for the elimination of the μ^{-2} term remains the same as above. The coefficient of μ^{-3} is equal to

$$d_3 = -\frac{8\,c_0\sqrt{\pi}}{27} + 2\,\alpha_0 \tag{50}$$

and is the same for all $l = 0$ states. The coefficient of μ^{-4} for $l = 0$ states is n-dependent. For $n = 1$ it is equal to

$$d_4 = \frac{1}{6} + \frac{64\,c_0}{81} - \frac{64\,\alpha_0}{9\sqrt{\pi}} + \frac{16}{27}\sqrt{\pi}\,c_0\,\alpha_0 - \frac{8\,\alpha_0^2}{3} \tag{51}$$

Solving equations $d_3 = d_4 = 0$ for c_0 and α_0, we obtain:

$$c_0 = \frac{27\,\alpha_0}{4\sqrt{\pi}}, \qquad \alpha_0 = \frac{8 \pm \sqrt{64 - 18\pi}}{12\sqrt{\pi}}. \tag{52}$$

This gives two possible solutions: $\{c_0 = 0.94364, \alpha_0 = 0.24778\}$ and $\{c_0 = 1.92115, \alpha_0 = 0.50446\}$. When we use either of these sets of parameters and expand the first-order correction to fourth order in $1/\mu$, we have:

$$1s: 0, \quad 2s: -\frac{1}{48\mu^4}, \quad 3s: -\frac{2}{81\mu^4}, \quad 2p: \frac{1}{6\mu^4},$$
$$3p: \frac{1}{9\mu^4}, \quad 3d: 0.$$

Thus, the error of the first-order correction to the eigenvalues is proportional to μ^{-4}.

References

1. Kohn W, Sham LJ (1965) Self-consistent equations including exchange and correlation effects. Phys Rev 140:A1133
2. Parr RG, Yang W (1994) Density-functional theory of atoms and molecules. Oxford University Press, Oxford
3. Ceperley DM, Alder BJ (1980) Ground state of the electron gas by a stochastic method. Phys Rev Lett 45:566
4. Perdew JP, Zunger A (1981) Self-interaction correction to density-functional approximations for many-electron systems. Phys Rev B 23:5048
5. Perdew JP, Wang Y (1992) Accurate and simple analytic representation of the electron-gas correlation energy. Phys Rev B 45:13244
6. Harris J, Jones RO (1974) The surface energy of a bounded electron gas. J Phys F Metal Phys 4:1170–1186
7. Langreth DC, Perdew JP (1975) The exchange-correlation energy of a metallic surface. Solid Sate Commun 17:1425–1429
8. Gunnarsson O, Lundqvist BI (1976) Exchange and correlation in atoms, molecules and solids by spin-density-functional formalism. Phys Rev B 13:4274–4298
9. Yang W (1998) Generalized adiabatic connection in density functional theory. J Chem Phys 109:10107–10110
10. Seidl M (2003) Density functional theory from the extreme limits of correlation. Int J Quantum Chem 91:145
11. Mori-Sánchez P, Cohen AJ, Yang W (2006) Self-interaction-free exchange-correlation functional for thermochemistry and kinetics. J Chem Phys 124:091102
12. Cohen AJ, Mori-Sánchez P, Yang W (2007) Assessment and formal properties of exchange-correlation functionals constructed from the adiabatic connection. J Chem Phys 127:034101
13. Colonna F, Savin A (1999) Correlation energies for some two- and four-electron systems along the adiabatic connection in density functional theory. J Chem Phys 110:2828
14. Pollet R, Colonna F, Leininger T, Stoll H, Werner H-J, Savin A (2003) Exchange-correlation energies and correlation holes for some two- and four-electron atoms along a nonlinear adiabatic connection in density functional theory. Int J Quantum Chem 91(2):84–93
15. Teale AM, Coriani S, Helgaker J (2009) The calculation of adiabatic-connection curves from full configuration-interaction densities: two-electron systems. J Chem Phys 130:104111
16. Teale AM, Coriani S, Helgaker J (2010) Range-dependent adiabatic connections. J Chem Phys 133:164112
17. Valance A, Bergeron H (1989) Model potentials or pseudopotentials: the connection via supersymmetry. J Phys B Mol Opt Phys 22:L65–L69
18. Lepage GP (1998) How to renormalize the Scrödinger equation. In: Barata JCA, Malbouisson APC, Novaes SF (eds) Particles and fields, proceedings of the ninth J.A. Swieca Summer School. World Scientific, Singapore
19. Savin A, Colonna F, Pollet R (2003) Adiabatic connection approach to density functional theory of electronic systems. Int J Quantum Chem 93:166–190
20. Toulouse J, Savin A, Flad H-J (2004) Short-Range exchange-correlation energy of a uniform electron gas with modified electron–electron interaction. Int J Quantum Chem 100:1047–1056
21. Taut M (1993) Two electrons in an external oscillator potential: particular analytic solutions of a Coulomb correlation problem. Phys Rev A 48:3561–3566
22. Karwowski J, Cyrnek L (2003) Two interacting particles in a parabolic well: Harmonium and related systems. Comput Methods Sci Technol 9(1–2):67–78

23 Jones W, March NH (1973) Theoretical solid state physics, vol 2. Dover, New York

24 Wolfram Research, Inc. (2016) Mathematica, Version 11.0, Champaign, IL